DNA AND CELL BIOLOGY
Volume 27, Number 12, 2008

Pp. 649–656
DOI: 10.1089/dna.2008.0733

Dynamic Intracellular Distribution of Eaf2 and Its Potential Involvement in UV-Induced DNA Damage Response

Fengfeng Zhuang,[1,2] Philip Yen,[1,2] Jiangyue Zhao,[1,3] Manuel Nguyen,[1]
Meisheng Jiang,[4] and Yi-Hsin Liu[1,2]

Eaf2 encodes a tumor suppressor that plays multiple functions in transcriptional activation, apoptosis, and embryonic development. In this study, we utilized GFP-EAF2 fusion protein to describe the dynamic subcellular movement of Eaf2. GFP-EAF2 is preferentially localized to the nucleus, and in the presence of ELL, it accumulates in nuclear speckles. However, Eaf2 is an unstable nuclear protein whose stability is affected by serum. Further, we provided first evidence that nuclear distribution of Eaf2 is responsive to DNA damage. Following UV irradiation, Eaf2 is relocalized to the nucleolus, suggesting a possible functional involvement of Eaf2 in DNA damage response.

Introduction

The cellular location of a protein provides important clues to its function. When a cell experiences genotoxic stress, it responds by mobilizing and directing stress-relieving machinery to various intracellular compartments to assist either in self-preservation or in inducing apoptosis (Tembe and Henderson, 2007). The nucleolus, well known for its role in rRNA synthesis and ribosome assembly, also partakes in other important regulatory functions, including DNA surveillance and repair (Zimber *et al.*, 2004; Tembe and Henderson, 2007). Most genotoxic stresses affect nucleolar structure and function as shown by dynamic movements of proteins in or out of the nucleolus in response to DNA damage. For example, UV irradiation causes the exodus of ARF, B23, and ribosomal subunits into the nucleoplasm and subsequent binding of ARF and B23 to mdm2. Sequestration of mdm2 by ARF and B23 binding leads to the stabilization of p53 and activation of DNA repair mechanism or apoptotic response (Lee *et al.*, 2005). Few other proteins have also been shown to move into the nucleolus in response to DNA damage. ING1 and PML are two documented examples. UV can induce ING1 expression and the movement of ING1 to the nucleolus to promote apoptosis (Helbing *et al.*, 1997; Scott *et al.*, 2001). Phosphorylation of PML causes its relocalization to the nucleolus where PML sequesters mdm2, thus helping to stabilize p53 (Bernardi *et al.*, 2004). Thus, recruitment of specific proteins to precise cellular compartments is considered a protective response to genotoxic stresses.

Eaf2 was initially discovered as a binding partner of ELL (polymerase elongation factor, 11–19 lysine rich gene) and an androgen-response gene whose expression is developmentally regulated during embryogenesis (Li *et al.*, 2003; Simone *et al.*, 2003; Xiao *et al.*, 2003). Eaf2's function as a potential regulator of transcription has been linked to its interaction with ELL to increase RNA polymerase II elongation activity (Kong *et al.*, 2005; Xiao *et al.*, 2006). This functional property of Eaf2 has drawn attention to its potential regulatory roles in various neoplastic disorders and in development. Overexpression of *Eaf2* induces apoptosis in prostate cancer cells lines and also suppresses xenograft tumor growth (Hahn *et al.*, 2007). Targeted deletion of *Eaf2* resulted in mice exhibiting high rates of lung adenocarcinoma, B-cell lymphoma, hepatocellular carcinoma, and prostate intraepithelial neoplasia (Xiao *et al.*, 2008). Additionally, *Eaf2* is required for eye development in the frog (Maurus *et al.*, 2005).

Theses previously documented functions of Eaf2, especially in carrying out its transcriptional coactivation function, would require its presence in the cell nucleus. By using GFP-Eaf2 fusion protein, we tracked intracellular trafficking of Eaf2 and identified functional domains that mediate its nuclear and intranuclear movement. Additionally, we showed that Eaf2 was specifically targeted to the nucleolus in response to UV irradiation, suggesting its potential role in DNA damage surveillance or repair.

[1]Department of Ophthalmology, Keck School of Medicine, University of Southern California, Los Angeles, California.
[2]Graduate Program in Craniofacial Biology, Center for Craniofacial Molecular Biology, School of Dentistry, University of Southern California, Los Angeles, California.
[3]Department of Ophthalmology, China Medical University, Shenyang, China.
[4]Department of Molecular and Medical Pharmacology, UCLA School of Medicine, Los Angeles, California.

Materials and Methods

Plasmid constructions

To construct serial deletions of *Eaf2*, cDNA fragments were amplified by performing PCR using specific primer pairs. PCR products were then cloned into the pDrive vector (Qiagen, Valencia, CA) and were subsequently inserted into pEGFP-c1 (Clontech, Palo Alto, CA). ELL-IRES-dsRed was constructed by inserting the ORF of ELL into the expression vector pIRES-dsRed, which was modified from pIRES-hrGFP-1a vector (Stratagene, La Jolla, CA) by the replacement of GFP with dsRed. ELL-Flag fusion expression plasmid was constructed by inserting ELL in-frame into p3xFlag, which was modified by removing the GFP from pIRES-hrGFP-1a vector. All DNA constructions were verified by sequencing.

Cell culture and DNA transfection

C2C12 mouse myofibroblasts were purchased from the American Type Culture Collections (Manassas, VA). Cells were cultured in DMEM supplemented with 10% fetal bovine serum (Hyclone, Logan, UT). C2C12 cells were seeded into 12-well plates 1 day before transfection. When the cells attained 60–80% confluence, transfections were performed using Lipofectamine Plus reagent (Invitrogen, Carlsbad, CA) according to existing transfection protocol (Zhuang and Liu, 2006). Each transfection was carried out in triplicate. To stain cell nuclei, Hochest 333342 in DMSO (Invitrogen) was added into the culture medium at a final concentration of 1 μg/mL and allowed to incubate for 1 h before observation.

Immunofluorescence

Twenty-four hours after transfection, C2C12 cells were fixed in 4% PFA for 10 min and washed with PBS. After blocking with 1% BSA, an anti-FLAG antibody (1:200 dilution, M2; Sigma-Aldrich, St. Louis, MO) or anti-B23 (1:100 dilution; Sigma-Aldrich) diluted in 1× PBS, 0.2% NP40, and 1% BSA was added into the well and incubated for 2 h at room temperature and was then washed three times with PBS. To probe for the primary antibodies, a goat anti-rabbit or a rabbit anti-mouse secondary antibody conjugated to rhodamine red (1:400 dilution; Molecular Probes, Eugene, OR) was added and incubated for 30 min. After cells were washed in PBS, fluorescence images were acquired using an Olympus inverted fluorescent microscope equipped with a SPOT CCD camera.

Western blot analysis

At the indicated time points after transfection, cells were collected and lysed for protein extraction and used for western blotting analysis. Protein concentration was determined by Bradford assay (Bio-Rad, Hercules, CA). Equivalent amounts of protein were fractionated on 10% SDS/PAGE and then electroblotted onto PVDF membranes (Pall Life Sciences, Ann Arbor, MI). After transfer, blots were probed with rabbit anti-GFP (Hypromatix, Worcester, MA) antibodies at a dilution of 1:1000, then incubated with a 1:10,000 dilution of horseradish peroxidase–conjugated anti-rabbit antibodies. Immuno-complexes were visualized using the chemiluminescence method according to manufacture's recommendations (Roche, Indianapolis, IN). Membranes were stripped and reprobed with an anti-Gapdh antibody (Chemicon, Temecula, CA) to verify protein loading.

UV irradiation and confocal microscopy

C2C12 cells were seeded on chamber slides on the day before transfection. GFP-EAF2 transfected cells were exposed to UV light of a 30 W germicidal lamp for 10 or 30 min, and irradiated cells were returned into the CO_2 incubator to allow recovery for 4 h before fixation. C2C12 cells were fixed in 4% PFA for 10 min and washed with PBS. After blocking with 1% BSA, an anti-B23 (1:100 dilution; Sigma-Aldrich) antibody diluted in 1× PBS, 0.2% NP40, and 1% BSA was added and incubated for 2 h at room temperature and was then washed three times with PBS. To probe for the primary antibodies, a rabbit anti-mouse secondary antibody conjugated to rhodamine red (1:400 dilution; Molecular Probes) was added and incubated for 30 min. After cells were washed in PBS, the chamber slide was mounted using mounting medium that contains DAPI (Vector Lab, Burlingame, CA). Fluorescent images were captured using a Zeiss LSM510 laser scanning confocal microscopy.

RT-PCR

Total RNA was isolated from GFP-EAF2–transfected C2C12 cells at 12-, 24-, 36-, and 48-h time intervals. Cells were harvested by trypsinization and collected as a pellet following centrifugation. RNA was extracted using the Trizol reagent (Invitrogen) according to the manufacturer's recommendation. DNAse I (Invitrogen) was added to the RNA sample to remove any genomic DNA contaminant. First-Strand cDNA were synthesized using the SuperScript III First-Strand Synthesis kit (Invitrogen). cDNAs were subjected to 30 amplification cycles. PCR products were fractionated on a 2% agarose gel. Resulting gel images were captured by using a Bio-Rad Gel Doc system (Bio-Rad).

Results

To examine cellular localization of Eaf2, we transiently transfected C2C12 myoblast cells with GFP-EAF2 fusion and GFP control expression plasmids. Normal GFP-transfected cells gave a stable GFP signal, while GFP-EAF2–transfected cells yielded a transient expression pattern. The full-length GFP-EAF2 exhibited nuclear localization 12 h after transfection (Figs. 1A and 2B). After 24 h, GFP fluorescence in the nucleus was still visible. However, 48 h later, there was no longer clear evidence of GFP within the nucleus (Fig. 1A), suggesting that Eaf2 is unstable. This was reconfirmed by performing western blot analysis (Fig. 1B). The expression of GFP-EAF2 fusion protein was examined at time intervals of 12, 24, 36, and 48 h after transfection. Two robust GFP-EAF2 protein bands were detected 12 h after transfection, and the detection signal became progressively weaker as time progressed. By 48 h, the GFP-EAF2 protein bands were barely detectable on the western blot, suggesting substantial destabilization or degradation (Fig. 1B). Cells transfected with the GFP control plasmid exhibited similar intensity of GFP fluorescence and virtually similar expression levels on the western blot during the entire time course (Fig. 1B). Inter-

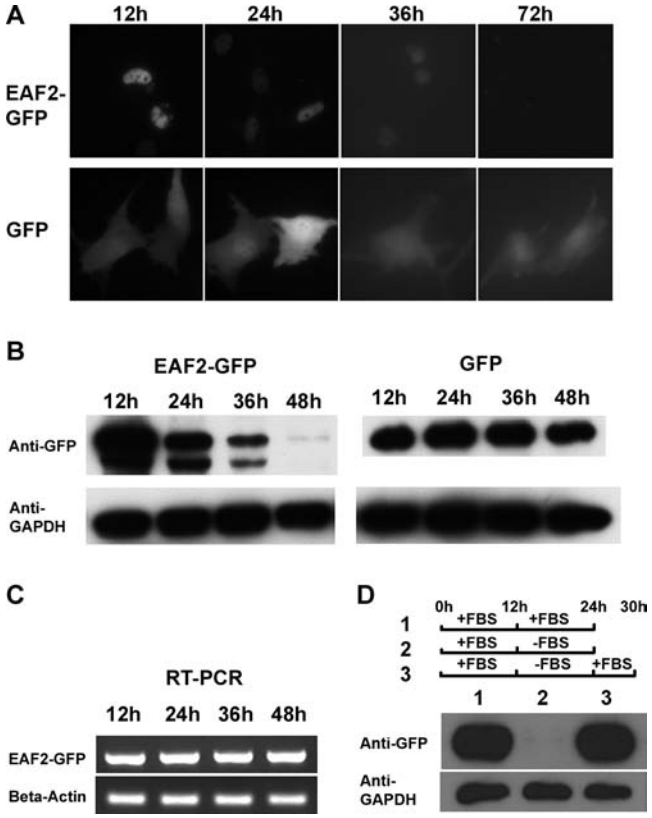

FIG. 1. Eaf2 is an unstable protein with a characteristic short half-life. (**A**) GFP-EAF2 fusion protein was exclusively localized in the cell nucleus 12 h after transfection. Degradation became evident beginning at 24 h posttransfection as the intensity of GFP-EAF2 fluorescence started to decrease. By 48 h after transfection, GFP-EAF2 fluorescence could no longer be detected, while control cells still emitted a strong GFP fluorescence. (**B**) Western blot analysis showed that GFP-EAF2 protein level gradually decreases as a function of time after transfection. This gradual decline in GFP-EAF2 protein level is consistent with the observed graduate reduction in the intensity of GFP fluorescence in (**A**). The protein level of GFP-EAF2 was barely detectable by 48 h after transfection, whereas the protein level in GFP controls remained steady. A rabbit anti-GFP antibody was used to detect GFP-EAF2 fusion protein. (**C**) RT-PCR was performed to detect GFP-EAF2 transcripts in transfected cells at indicated time points. Coamplification of *β-actin* was used as control. No difference in GFP-EAF2 transcript levels was detected at any indicated time points after transfection. (**D**) Within 24 h of culturing period in the growth medium (+FBS), the level of GFP-EAF2 fusion protein remained relatively abundant as shown on the Western blot (lane 1). Serum starvation (−FBS) resulted in a dramatic disappearance of the GFP-EAF2 fusion protein (lane 2). GFP-EAF2 was restabilized when serum-containing culture medium (+FBS) was reintroduced for 6 h (lane 3).

estingly, we detected two distinct protein species: a predicted 56 KDa band and a slower migrating 60 KDa band (Fig. 1B). The larger protein species may be a product of posttranslational modification. To demonstrate that the decrease in GFP-EAF2 protein level was a result of protein degradation, PCR was performed on reverse transcribed cDNA to show that the level of GFP-EAF2 transcripts did not change during the time course following transfection (Fig. 1C). The stability of GFP-EAF2 protein is also vulnerable to serum starvation. When GFP-EAF2–transfected cells were grown in medium without serum for 12 h, EAF-GFP proteins were totally degraded. An addition of fresh serum into serum-starved culture for 6 h stimulated new synthesis and accumulation of EAF-GFP (Fig. 1D).

To identify the domain required for Eaf2 nuclear translocation, we made serial truncations of Eaf2 fusion with GFP and transfected them into C2C12 cells (Fig. 2A). All truncated GFP-EAF2 constructs showed the same pattern of diffuse cytoplasmic expression, and poor nuclear localization with varying degrees of regional preference, except for the EAF2-NM (aa 1–163) C-terminal deletion construct (Fig. 2B). The EAF2-N (aa 1–86) mutant exhibited a diffuse pattern of expression throughout the cytoplasm with no evidence of localization to a specific subcellular location. The EAF2-M mutant (aa 86–163) showed diffused cytoplasmic distribution pattern. The EAF2-C mutant (aa 163–262) again showed a diffused cytoplasmic localization pattern. The EAF2-MC truncation (aa 86–262) exhibited a similar pattern. The EAF2-NM (aa 1–163) truncation showed clear nuclear localization, suggesting that the region required for nuclear localization lies within this protein domain (Fig. 2B).

Presence of Eaf2 in the cytoplasm following degradation in the nucleus

Although the GFP-EAF2 was barely detectable in the nucleus 48 h after transfection, we detected a ring of GFP-EAF2 fluorescence surrounding the cell nucleus at 72 h after transfection (Fig. 2B). This indicates that a portion of the Eaf2 protein was either exported from the nucleus to the cytoplasm or newly synthesized GFP-EAF2 fusion proteins were retained in the cytoplasm (Fig. 2B). This cytoplasmic retention phenomenon was also observed with GFP-EAF2 truncation mutants. Each of the truncation mutants, except for the EAF2-NM and EAF2-N, exhibited similar patterns of nuclear exclusion as the wild-type GFP-EAF2 at 72 h posttransfection (Fig. 2B).

ELL-induced subnuclear relocalization of Eaf2 is mediated by its C-terminal domain

Transient cotransfection of Eaf2 with ELL causes relocalization of Eaf2 into nuclear speckles (Fig. 3A). In cells that were transfected with GFP-EAF2 alone, we observed a diffuse pattern of GFP fluorescence throughout the nucleus. In the cells that were cotransfected with GFP-EAF2 and FLAG-tagged ELL, we observed dual fluorescence exclusively in nuclear speckles, indicating that the Eaf2 relocalization was mediated by ELL. The C-terminal domain of Eaf2 (EAF2-C, aa 163–262) alone was sufficient for targeting the fusion protein to nuclear speckles in the presence of cotransfected ELL-IRES-dsRed (Fig. 3B). In contrast to a previous study in which the ELL interaction domain was mapped to the amino-terminus of Eaf2 (Simone *et al.*, 2003), our results demonstrated that nuclear speckle formation of Eaf2 does not require ELL binding domain, suggesting that ELL may play a role in activating an inductive signal to facilitate the appearance of Eaf2 nuclear speckles.

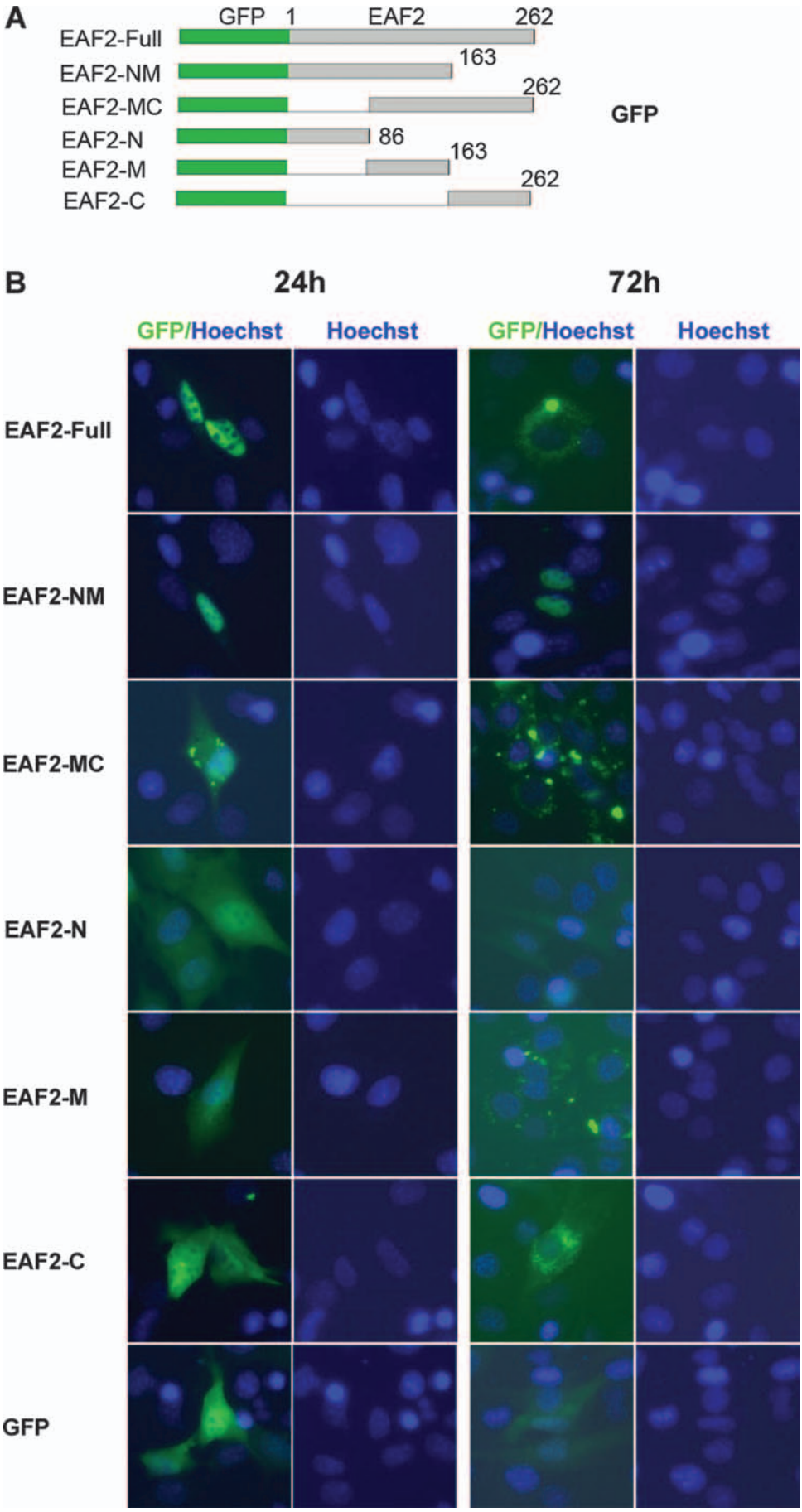

FIG. 2. Nuclear localization of Eaf2 does not rely on its C-terminus (**A**). Schematic representation of GFP fused in-frame to various Eaf2 deletions. (**B**) Full-length and truncated GFP-EAF2 fusion expression plasmids were transfected into C2C12 cells and visualized using fluorescent microscopy to detect GFP. Only the EAF2-NM deletion mutant exhibited the same pattern of nuclear localization as the wild-type Eaf2 (EAF2-Full). All other Eaf2 deletion mutants showed fluorescence predominantly in the cytoplasm besides the nucleus (Hoechst 33342). After 72 h, GFP-EAF2 deletion derivatives were mostly excluded from the cell nucleus and exhibited limited cytoplasmic distribution surrounding the nuclear membrane, while the GFP control displayed a diffused fluorescence pattern at 24 or 72 h after transfection. Color images available online at www.liebertonline.com/dna.

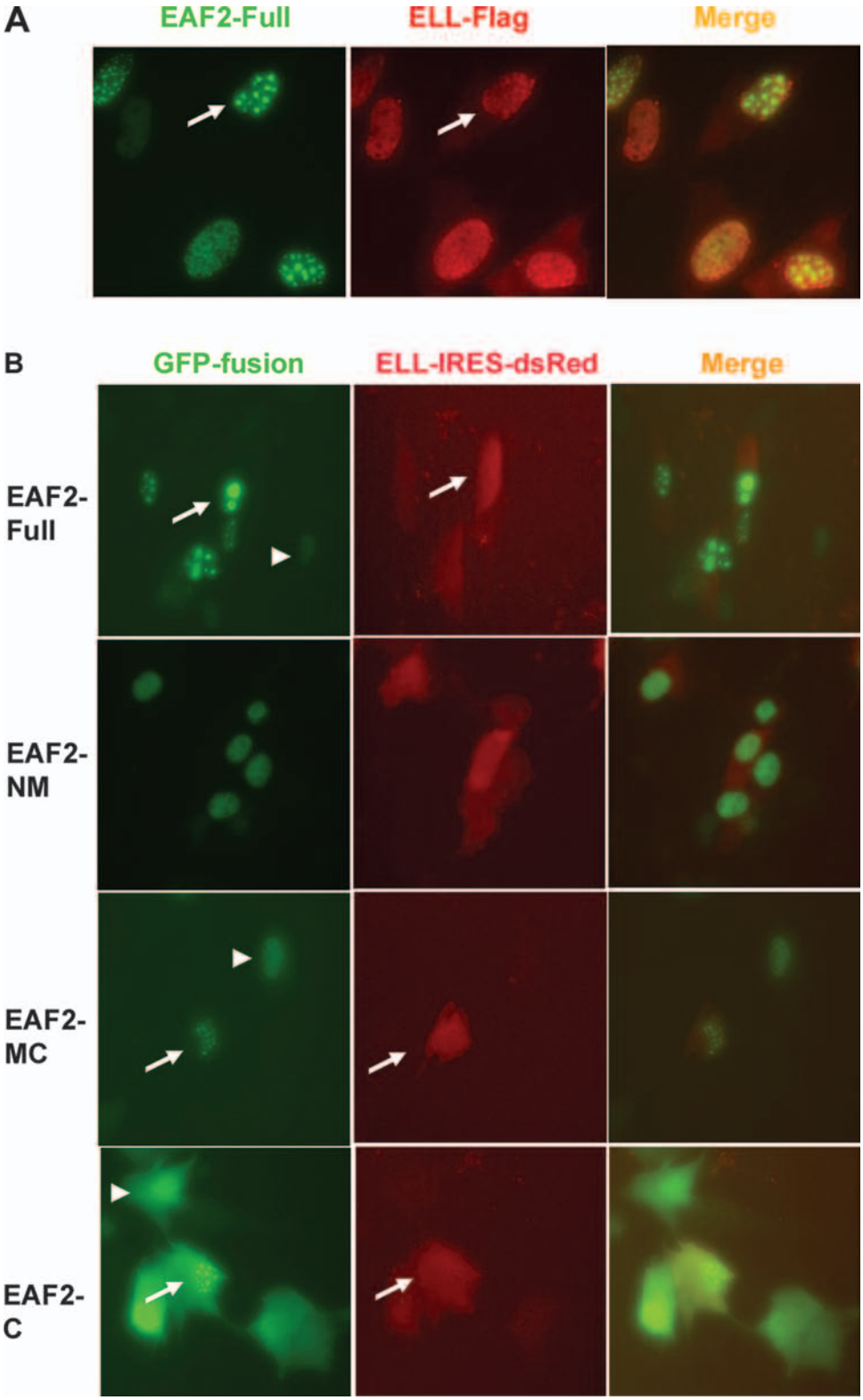

FIG. 3. EAF2 is relocalized into nuclear speckles in the presence of ELL. (**A**) Eaf2 colocalized with ELL in the cell nucleus. GFP-EAF2 and FLAG-tagged ELL expression vectors were cotransfected into C2C12 cells. ELL was visualized by immunofluorescence using the anti-FLAG antibody and a secondary antibody conjugated to Rhodamine. GFP-EAF2 accumulated in nuclear speckles when coexpressed with ELL (arrows). (**B**) The relocalization of GFP-EAF2 to nuclear speckles would only occur in the presence of an intact Eaf2 C-terminal domain. GFP-EAF2 wild type and truncation mutants were cotransfected with ELL-IRES-DsRed into C2C12 cells. The N-terminal deletion mutants (EAF2-MC and EAF2-C) were capable of targeting GFP to nuclear speckles only in the presence of cotransfected ELL (arrows), while removal of the C-terminal domain from EAF2 (EAF2-NM) resulted in a diffused nuclear distribution pattern. In the absence of ELL coexpression, GFP-EAF2 and Eaf2 mutants failed to show fluorescence in nuclear speckles (arrowheads). Color images available online at www.liebertonline.com/dna.

UV irradiation triggers the relocalization of Eaf2 into the nucleolus

Several proteins involved in DNA repair change their intracellular localization and form DNA repair foci following DNA damage (Helbing *et al.*, 1997; Scott *et al.*, 2001; Kurki *et al.*, 2003; Bernardi *et al.*, 2004; Zimber *et al.*, 2004; Lee *et al.*, 2005; Tembe and Henderson, 2007). To investigate the possibility that EAf2 may play a role in response to genotoxic stress, we exposed GFP-EAF2–transfected C2C12 cells to UV irradiation for 30 min to induce DNA damage. UV-irradiated

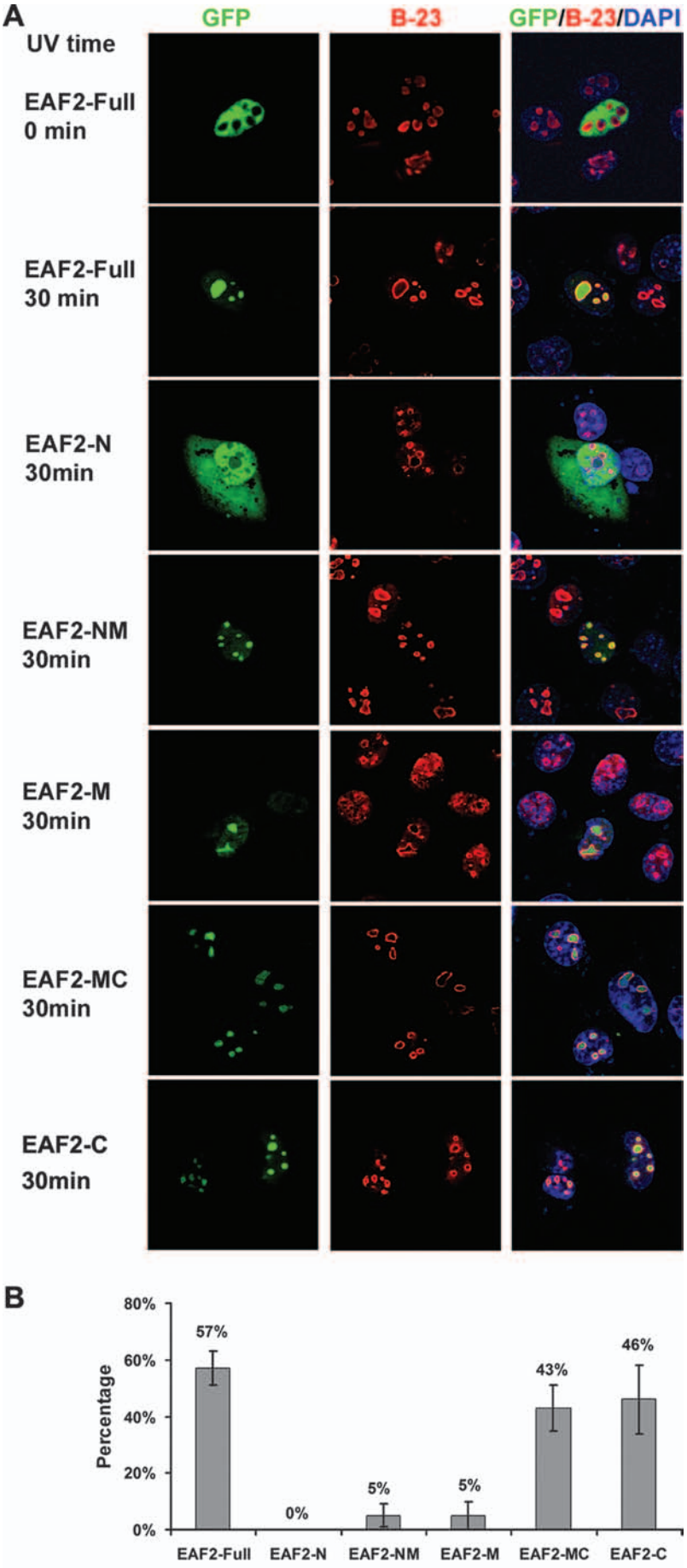

FIG. 4. Eaf2 is targeted to the nucleolus after UV irradiation. (**A**) C2C12 cells transfected with GFP-EAF2 or various GFP-EAF2 deletion mutants were exposed to UV irradiation for up to 30 min, and then were allowed to recover in growth medium for 4 h. Cells were then fixed for immunofluorescence detection of nucleoli with a monoclonal anti-B23 primary antibody and a secondary anti-mouse IgG antibody that has been conjugated to rhodamine. In the absence of UV damage, the full-length GFP-EAF2 failed to form nuclear foci, while GFP fluorescence was found only in the nucleus (blue DAPI stain). After a 30-min exposure to UV light, GFP-EAF2 relocated into B23-positive nucleoli. The N-terminus EAF2-GFP mutant (EAF2-N) was excluded from the nucleolus, while other Eaf2 mutant proteins were all capable of shuttling into nucleoli. (**B**) The percentage represents the percentage of cells in which GFP and B23 were colocalized after UV irradiation. Both the center portion of the Eaf2 and its C-terminus contain sufficient sequence information to target GFP-EAF2 into the nucleolus. However, the preferred nucleolus-targeting signal is harbored within the C-terminus domain of Eaf2, so that EAF2-MC and EAF-C GFP fusion proteins are more efficient in nucleoli translocation. Color images available online at www.liebertonline.com/dna.

cells were then allowed to recover for 4 h. Intriguingly, GFP-EAF2 emitted fluorescence from distinct nuclear compartments in cells that received UV exposure (Fig. 4A), while cells that were not exposed to UV irradiation showed the expected diffuse GFP-EAF2 fluorescence in their nuclei, and GFP fluorescence was excluded from nuclear compartments that appeared to be nucleoli. In cells exposed to 10 min of UV irradiation, we observed little to no change in the GFP-EAF2 distribution pattern; although some faint GFP fluorescence was evident in nuclear foci (data not shown). To determine the nature of UV-induced nuclear foci, we performed immunofluorescence using an anti-B23 antibody that specifically detects nucleoplasmin in the nucleolus. While GFP-EAF2 was specifically excluded from B23-positive nucleolus in the absence of UV treatment, GFP-EAF2 was colocalized with B23 in the nucleolus following UV irradiation (Fig. 4A). To determine specific functional domain(s) that mediates nucleolar translocation, various GFP-EAF2 deletion constructs were transfected into the cell. Following a 30-min UV irradiation and a recovery period of 4 h, transfected cells were fixed and stained using the anti-B23 antibody. The number of cells that showed colocalization of GFP with B23 was tallied. With the exception of EAF2-N, all other Eaf2 truncation mutants exhibited GFP fluorescence in the nucleolus with different efficiencies. About 43% to 46% of the cells that were transfected by EAF2-MC or EAF2-C exhibited intense GFP fluorescence in their nucleoli, while fewer than 5% of the cells transfected by either EAF2-NM or EAF2-M showed GFP-positive nucleoli, respectively (Fig. 4B). The efficiency of nucleoli translocation displayed by the EAF2-MC and EAF2-C constructs closely resembles the full-length wild-type Eaf2 (Fig. 4B). Thus, this UV-induced redistribution of Eaf2 was mediated by the Eaf2 central domain and its C-terminal domain. The C-terminal domain (EAF2-C, aa 163–262) alone was sufficient to target GFP to nucleoli (Fig. 4A, B).

Discussion

In this report we demonstrated that Eaf2 is an unstable nuclear protein. It appears that the stability of Eaf2 is sensitive to factor(s) in the serum because serum starvation resulted in its rapid degradation, whereas addition of fresh medium resulted in its quick accumulation. The fusion protein was degraded and removed from the cell nucleus as demonstrated by the progressively diminishing GFP fluorescence in GFP-EAF2–transfected cells and by a gradual reduction in the GFP-EAF2 protein level on western blots. Its subsequent reappearance—though at very low levels—was found exclusively in the cytoplasm encircling the nuclear membrane, forming a ghost image of the nucleus. It is possible that prior nuclear accumulation of Eaf2 may have evoked a negative feedback mechanism, perhaps via ubiquitination, that resulted in the degradation of Eaf2 prior to its importation into the nucleus. This is consistent with our finding that a larger than predicted protein band was detected on the western blot. This slower migrating GFP-EAF2 fusion protein may be the product of posttranslational modification, such as ubiquination. Further investigation is necessary to reveal the nature of this modification and to uncover the exact mechanism of cytoplasmic retention/degradation of Eaf2.

By deletion analysis, we further showed that the nuclear targeting signal resided between amino acid residues 1 and 163 in the N-terminal domain of Eaf2. Only the full-length Eaf2 and the Eaf2 truncation mutant that carries the entire 163 amino acid residues exhibited unambiguous and exclusive green fluorescence in the cell nucleus. Interestingly, this same domain was previously shown to physically interact with ELL (Simone *et al.*, 2003; Hahn *et al.*, 2007). Under the normal physiological condition, Eaf2 is present in the nucleus in a diffused pattern. When coexpressed with ELL, Eaf2 accumulates and colocalizes with ELL in small nuclear bodies. The C-terminal domain (aa 163–262) provides sufficient information to achieve this intranuclear targeting event. This is in contrast to the finding that ELL interacting domain (aa 36–113) was required for targeting Eaf2 to nuclear speckles in Cos-7 cells (Xiao *et al.*, 2006). It is possible that differences in cellular contexts and differences between the human and mouse Eaf2 at the sequence level may have contributed to this discrepancy.

Intriguingly, genotoxic stress could also trigger relocalization of Eaf2. We showed that when cells were exposed to UV irradiation, Eaf2 was relocalized into the nucleolus, suggesting that Eaf2 may play a functional role in the nucleolus, such as in sensing and repairing DNA damage or in triggering apoptosis. This unique property of intranuclear movement is strikingly similar to that shown by ING1 following UV irradiation (Scott *et al.*, 2001; Soliman and Riabowol, 2007). Interestingly, the domain that mediates nucleolar targeting is also located in the C-terminus of Eaf2. This domain is a serine-rich region that can be potentially phosphorylated. This same domain was previously shown to activate transcription (Xiao *et al.*, 2006). Further analysis of its interacting partner(s) and the nature of posttranslational modification(s) will definitely provide clues to mechanisms of Eaf2 function.

Acknowledgments

The authors thank Susan Clarke and Angela Liu for providing editorial support. This work was supported in part by the National Institutes of Health grants DE12941 and EY015417.

Disclosure Statement

No competing financial interests exist.

References

Bernardi, R., Scaglioni, P.P., Bergmann, S., Horn, H.F., Vousden, K.H., and Pandolfi, P.P. (2004). PML regulates p53 stability by sequestering Mdm2 to the nucleolus. Nat Cell Biol **6,** 665–672.

Hahn, J., Xiao, W., Jiang, F., Simone, F., Thirman, M.J., and Wang, Z. (2007). Apoptosis induction and growth suppression by U19/Eaf2 is mediated through its ELL-binding domain. Prostate **67,** 146–153.

Helbing, C.C., Veillette, C., Riabowol, K., Johnston, R.N., and Garkavtsev, I. (1997). A novel candidate tumor suppressor, ING1, is involved in the regulation of apoptosis. Cancer Res **57,** 1255–1258.

Kong, S.E., Banks, C.A., Shilatifard, A., Conaway, J.W., and Conaway, R.C. (2005). ELL-associated factors 1 and 2 are positive regulators of RNA polymerase II elongation factor ELL. Proc Natl Acad Sci USA **102,** 10094–10098.

Kurki, S., Latonen, L., and Laiho, M. (2003). Cellular stress and DNA damage invoke temporally distinct Mdm2, p53 and PML

complexes and damage-specific nuclear relocalization. J Cell Sci **116,** 3917–3925.

Lee, C., Smith, B.A., Bandyopadhyay, K., and Gjerset, R.A. (2005). DNA damage disrupts the p14ARF-B23(nucleophosmin) interaction and triggers a transient subnuclear redistribution of p14ARF. Cancer Res **65,** 9834–9842.

Li, M., Wu, X., Zhuang, F., Jiang, S., Jiang, M., and Liu, Y.H. (2003). Expression of murine ELL-associated factor 2 (*Eaf2*) is developmentally regulated. Dev Dyn **228,** 273–280.

Maurus, D., Heligon, C., Burger-Schwarzler, A., Brandli, A.W., and Kuhl, M. (2005). Noncanonical Wnt-4 signaling and EAF2 are required for eye development in *Xenopus laevis*. EMBO J **24,** 1181–1191.

Scott, M., Boisvert, F.M., Vieyra, D., Johnston, R.N., Bazett-Jones, D.P., and Riabowol, K. (2001). UV induces nucleolar translocation of ING1 through two distinct nucleolar targeting sequences. Nucleic Acids Res **29,** 2052–2058.

Simone, F., Luo, R.T., Polak, P.E., Kaberlein, J.J., and Thirman, M.J. (2003). ELL-associated factor 2 (EAF2), a functional homolog of EAF1 with alternative ELL binding properties. Blood **101,** 2355–2362.

Soliman, M.A., and Riabowol, K. (2007). After a decade of study-ING, a PHD for a versatile family of proteins. Trends Biochem Sci **32,** 509–519.

Tembe, V., and Henderson, B.R. (2007). Protein trafficking in response to DNA damage. Cell Signal **19,** 1113–1120.

Xiao, W., Jiang, F., and Wang, Z. (2006). ELL binding regulates U19/Eaf2 intracellular localization, stability, and transactivation. Prostate **66,** 1–12.

Xiao, W., Zhang, Q., Habermacher, G., Yang, X., Zhang, A.Y., Cai, X., Hahn, J., Liu, J., Pins, M., Doglio, L., Dhir, R., Gingrich, J., and Wang, Z. (2008). *U19/Eaf2* knockout causes lung adenocarcinoma, B-cell lymphoma, hepatocellular carcinoma and prostatic intraepithelial neoplasia. Oncogene **27,** 1536–1544.

Xiao, W., Zhang, Q., Jiang, F., Pins, M., Kozlowski, J.M., and Wang, Z. (2003). Suppression of prostate tumor growth by U19, a novel testosterone-regulated apoptosis inducer. Cancer Res **63,** 4698–4704.

Zimber, A., Nguyen, Q.D., and Gespach, C. (2004). Nuclear bodies and compartments: functional roles and cellular signalling in health and disease. Cell Signal **16,** 1085–1104.

Zhuang, F., and Liu, Y.H. (2006). Usefulness of the luciferase reporter system to test the efficacy of siRNA. Methods Mol Biol **342,** 181–187.

Address reprint requests to:
Yi-Hsin Liu, Ph.D.
Department of Ophthalmology
Keck School of Medicine
University of Southern California
1355 San Pablo St., DVRC314
Los Angeles, CA 90033

E-mail: yhliu@usc.edu

Received for publication January 14, 2008; received in revised form August 5, 2008; accepted August 8, 2008.